Robot-Assisted Surgery on Soft Tissue Dynamics

Felix Cruz[1], David Hoang[1], Shannon Lin[1], and Andrew Setiadi[1]

***Abstract*— In recent years, robotic surgery and robotic-assisted surgery (RAS) has become popularized as a means of performing surgery that accounts for limitations in conventional surgical methods and introduces robot-enhanced approaches. However, one known issue that arises with the use of robotic arms is unwanted oscillations due to certain material properties of the components of the machine, such as stiffness. Thus, it is critical that the information input by the operator (i.e. surgical motions) is relayed properly to the robot, and that appropriate information is relayed back to the operator to replicate a conventional surgical environment. In this project, we aim to examine the controller-arm system, wherein the input is the operator's movement and the output is the arm movement, and design a PID controller that will help greatly reduce steady state error, remove any oscillations, and have a fast response while maintaining stability.**

I. Introduction

A. Robotic-Assisted Surgery

Robotic-assisted surgery (RAS) encompasses a broad range of procedures in which robotic arms functioning as surgical instruments are tele-controlled by a surgeon either through tele-manipulation or computer control. RAS has advanced rapidly in the past couple of decades, allowing surgeons to surpass the limitations of traditional surgical procedures by improving dexterity, precision, and accuracy of movement as well as increasing accessibility to harder to reach areas in the body while decreasing disruption of surrounding areas. The growing popularity and prevalence of these robotic procedures can be attributed to the increased demand and diversification of minimally invasive surgery techniques. RAS has allowed for many common surgeries to be much more minimally invasive, resulting in increased recovery rates and times as well as decreased scarring and pain for patients.

In general, RAS incorporates three components: the robotic instrument, the processing equipment, and the control console used by the surgeon to command the robot [1]. Depending on their intended application, these robotic instruments can vary widely in complexity, differing in the types and amounts of joints, the allowable degrees of freedom (DOF) of those joints, the end effector used to interact with the contact environment, and the workspace size. Controlling a robot to move to desired positions or provide desired force outputs has many inherent sources of error, such as oscillations due to momentum or material properties of the robotic links [2]. For RAS, an important additional source of error to account for as the contact environment changes from hard, solid, and static surfaces to soft, flexible, and unfixed surfaces such as biological tissues is how the contact environment will react to the manipulation. Surgical contact environments often involve different biological tissue types with different mechanical properties such as nonlinearity and elasticity, which cause them to produce reactive force when subject to applied forces. While the design of a robot for RAS is constrained by aspects such as material biocompatibility, engineers can still manipulate properties of the robot to make them highly optimized. In comparison, we have very limited capabilities to change the properties of the contact environments to increase workability. However, we do have the ability to control how the robot behaves as it interacts with the contact environment. Thus, to account for possible sources of error from both the robotics and contact environment in real time, and assuming the robot is well suited for the application and controlled by a well trained surgeon, force and position feedback control must be implemented.

Since these robots are implemented in such a delicate and sterile environment, force outputs must be accurate and precise enough to be deemed safe and efficient. This requires appropriate force applications and positioning relative to a defined contact environment such as the soft tissue of humans. This, however, poses issues because soft tissues are not purely solid, static, or perfectly elastic, making proposed models limited in what they can predict in the operating room. Additionally, robotic systems are limited as surgeons cannot feel the intricate environment they are working in nor the robotic effect on the soft tissue which traditionally informs surgeons on how to change their course of action. This suggests the potential improvement of modeling robotic systems in surgery through the inclusion of haptic or tactile feedback to reduce errors associated with the robotic movement.

II. Biosystem

A typical RAS system can be modeled as several key components, which are summarized in Figure 1. The surgeon inputs a motion and force which is sent to the master manipulator, commanding the patient-side manipulator to interact with the patient. In return, the force and tissue properties provide tactile and force information to the tactile display/master manipulator, which gives a kinesthetic and cutaneous sense to the surgeon. In addition, an endoscope outputting video data to a graphical display provides visual feedback for the surgeon.

Our project focuses on the interaction between the robot end-effector and the patient, specifically the force feedback system that allows for the end-effector to exert a desired

[1]Department of Bioengineering, Jacobs School of Engineering, UC San Diego, La Jolla, CA 92093, USA.

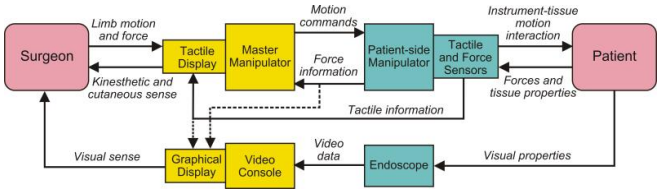

Fig. 1. Schematic diagram of a typical RAS system. Important components include the motion commands given by the master manipulator and the force information being returned by the patient-side manipulator. Adapted from [3]

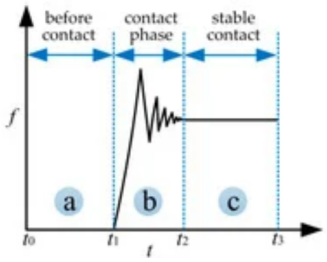

Fig. 2. Time-domain diagram of the force response at different stages of contact, where a) is before contact, b) is initial contact, and c) is stable contact. Adapted from [4]

force input by the surgeon. The components of this system include the robot arm mechanics, the contact environment behavior, and a controller to minimize output error and/or oscillations. In the operating room, this is critical for ensuring that the end-effector does not exert unnecessary forces upon the contact environment. Figure 2 shows the force output of the end-effector when contact is initiated, with steadily decaying oscillations occurring from the time of contact until stability is reached. These initial oscillations are undesired force outputs, and thus need to be reduced or removed using a controller.

In addition to force control, there is also an internal position feedback loop for the robot arm mechanics. Accounting for the position of the end-effector is equally important as the force, as position feedback can ensure that the surgeon is operating on the correct locations for a given tissue. Such position feedback is even more important if the area of interest is relatively small, requiring minute and precise surgical actions. It is important to note that there are a few operational constraints, mainly how generated force and position values are limited by the base programming and mechanics of the robot. That is, there is a physical limitation to how quickly and precisely the end-effector is able to be adjusted.

III. Methods

A. Key Assumptions

In order to simplify the modelling and simulation process, several key assumptions have been made. Firstly, we assume that the robotic end-effector has only one translational degree of freedom, such as a needle moving vertically perpendicular to the tissue. We will also assume that the robot arm can be modelled using a mass-spring-damper system [4]. While this might be less appropriate for a system with multiple degrees of freedom, this model fits under the previous assumption. For the contact environment that the end-effector interacts with, we assume that it is a static, viscoelastic, homogeneous, and isotropic soft tissue. In regards to the overall system model, measurements of the output force will be treated as ideal with no time delay in the measurements. This simplification makes it easier to simulate the system; in reality measurement delay would have a notable impact on the system output and require different controller tuning. In a similar vein, we assume that the initial conditions are zero, where the end-effector is in contact with the environment but no force is applied. Finally, we assume that the surgeon/operator must input slow movements (i.e. low frequency changes) with low force values, meaning our domain of interest is within small frequencies and forces.

B. Mathematical Modelling

The simplification of the robot arm to a mass-spring-damper system is derived as follows. Firstly, the relationship between position and velocity can be expressed as shown in Eq. 1. In addition, the sum of forces on the mass are accounted for in Eq. 2, which shows the influence of the spring, damper, and any external forces where γ is the damping constant, k is the spring constant, and m is the mass.

$$\frac{du}{dt} = v(t) \tag{1}$$

$$m\frac{dv}{dt} = -\gamma v(t) - ku(t) + f(t) \tag{2}$$

Using both equations results in a single second-order differential equation (3), which, after applying a Laplace transformation, results in the transfer function (4) where the input and output are force and position, respectively.

$$m\frac{d^2u}{dt^2} = -\gamma\frac{du}{dt} - ku(t) + f(t) \tag{3}$$

$$\frac{U(s)}{F(s)} = \frac{1}{ms^2 + \gamma s + k} \tag{4}$$

Unfortunately, no explicit parameters regarding robotic mechanisms for this model were found in current literature. While there seemed to be a few related values in papers regarding robot arm modelling, it was difficult to find anything that matched our system. Thus, we made an educated guess and set γ = 100 Ns/m, k = 300 N/m, and m = 0.01 kg (approximately the mass of a hypodermic needle).

As for the contact environment, the viscoelasticity of soft tissue is traditionally represented through a variety of spring-damper systems. For this project, we opted for the Kelvin-Boltzmann model, which was found to be best representative of a dynamic soft tissue force response in a study by Morieria et. al regarding soft tissue force control [5]. The Kelvin-Boltzmann model (5) contains two springs and one damper, expressed through the parameters α, β, and γ (6).

$$F(t) = \beta x(t) + \alpha\dot{x}(t) - \gamma\dot{F}(t) \tag{5}$$

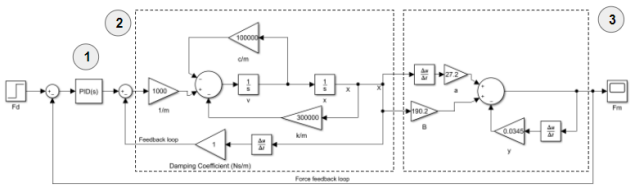

Fig. 3. SIMULINK block diagram of the overall system, where (1) is the PID controller, (2) is the robotic arm mechanics, and (3) is the soft tissue mechanics.

$$\alpha = b\frac{k_2}{k_1+k_2}, \beta = \frac{k_1 k_2}{k_1+k_2}, \gamma = \frac{b}{k_1+k_2} \tag{6}$$

β is best representative of the tissue stiffness, and α, γ are both related to tissue viscosity. By performing a Laplace transform on (5), a transfer function for the Kelvin-Boltzmann model can be obtained (7), where the input and output are position and force, respectively:

$$\frac{F(s)}{X(s)} = \frac{1+\gamma s}{\beta+\alpha s} \tag{7}$$

Values for the soft tissue model were also obtained from the study by Morieria et. al, which were experimentally determined using beef as the tissue of choice. In this case, α = 27.2 Ns/m, β = 190.2 N/m, and γ = 0.0345 s. While these parameters are appropriate given our assumptions (i.e. examining interaction with any soft tissue in general), it is important to note that a more specific scenario would require different parameters to be more accurate. Furthermore, because we have assumed that the contact environment is homogeneous, we are not considering differences in tissue composition. Human skin, for example, is layered with tissues that vary in their physical properties that would need to be accounted for in a more robust simulation.

C. SIMULINK

In accordance with our prior description of the biosystem of interest for this project, a block diagram representing all of the components of the biosystem was generated in SIMULINK (Figure 3). The force input, F_d, is modeled as a step function and compared with the measured force, Fm; the resulting difference is fed into the PID controller. This force is then input into a system representing the robot arm mechanics, which outputs a resulting position for the arm. Note that there is a position feedback loop that works by converting the output position into a force by deriving the position into a velocity and multiplying it with a damping coefficient in units of Ns/m.

The position output generated by the robot arm then acts as the input for the soft tissue mechanics (Kelvin-Boltzmann model), yielding a final measured force F_m that acts as the overall force feedback loop as mentioned earlier. Values for the PID controller were determined using the built-in SIMULINK PID tuner, which yielded values of K_P = 2.092, K_I = 12.64, and K_D = -0.0229. As per the assumptions mentioned previously, the force inputs that we tested for were kept at low values: F_d= 0.1 N, 0.5 N, and 1 N. Afterwards,

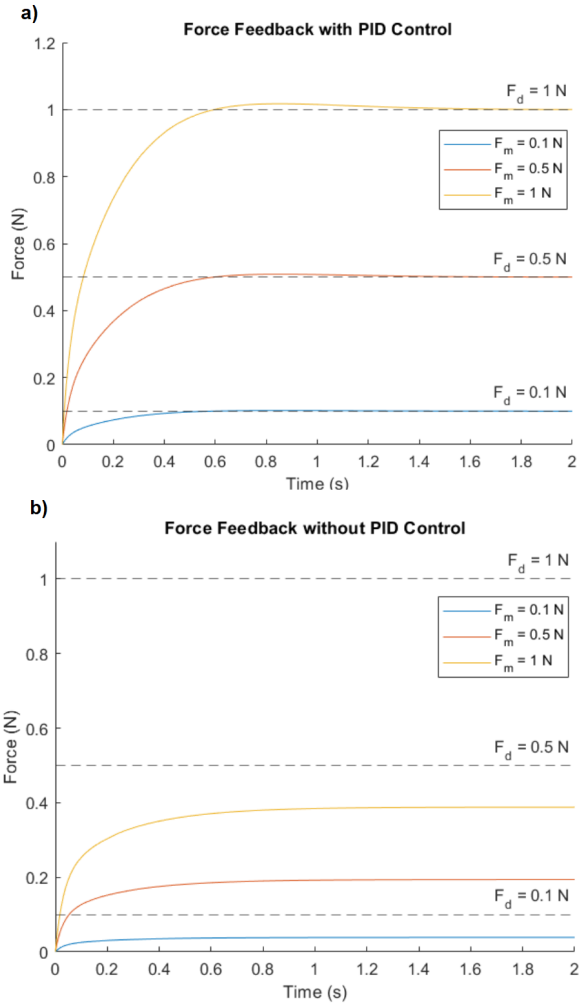

Fig. 4. System force response for varying force input values. Dashed lines indicate the desired steady-state value Fd, and each curve represents the measured force, Fm. a) shows the force responses for the closed-loop system with PID control, whereas b) shows the responses when PID control is removed.

a frequency response analysis was performed by plotting a bode diagram using the SIMULINK linearization toolbox.

IV. Results and Analysis

A. Time-domain Response

Running the SIMULINK simulation for different small-value forces resulted in the outputs summarized in Figure 4a. All curves appear to be similar in behaviour, with no oscillations and minimal overshooting. More importantly, compared to Figure 4b, the steady-state gain error has been greatly reduced with the inclusion of the PID controller.

While the steady-state errors without PID control (Figure 4b) are at 61.2%, adding a PID controller drastically reduces the percent error to 0.01%. Visually, there does not seem to be a large difference in settling time between the two cases. There is some overshoot present before the force reaches steady-state with the PID controller; however, the percentage

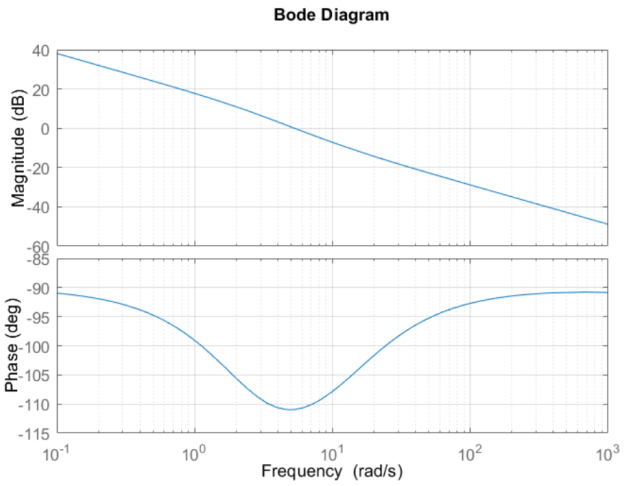

Fig. 5. Bode diagram of the closed-loop system.

overshoot is only 1.74%. Thus, from the perspective of the force response, the closed-loop can be considered stable.

B. Frequency Response

Because we are only concerned with low-frequency changes in the input force, the bode plot (Figure 5) is examined at a range of 10^{-1} rad/s to 10^{3} rad/s. Within this range, it is apparent that for higher frequencies, lower gain values are observed (starting at 5 rad/s). This implies that for any rapid changes in force input, the resulting output will be reduced. In addition, the phase margin is 70° and the gain margin is infinite, as the system does not reach a phase angle of -180° within this frequency range.

The results of the bode diagram thus further verify the stability of the closed-loop system, and validate the use of a PID controller to fix steady-state error with minimal overshooting.

V. Discussion

One major area of improvement for our simulation is in regard to modelling the robot dynamics. In our block diagram, such dynamics were modelled as a spring-mass-damper system. However, not all robotic systems can be simplified as such. Some of the existing literature that we researched for this project considered multiple degrees of freedom, accounting for other factors like Coriolis and centripetal forces. Additionally, as mentioned prior, we found no obvious parameters for the constant values needed for the spring-mass-damper system in the literature. These values were chosen based on an estimated guess, and thus may not accurately represent reality.

For the scope of our project, we decided that a system with the highest accuracy (i.e. lowest steady-state error) would be ideal. The PID controller was determined to be the best design for such since it resulted in a substantially lower steady-state error compared to other controllers that we tested for, namely P and PI controllers. The PID controller is also able to reduce these errors without compromising the settling time and introducing extreme overshoot. However, the P controller had a significantly lower settling time and no overshoot compared to both the PI and PID controllers. In the case where a low settling time free of any overshoot is desired, the P controller would be more optimal.

A major advantage of using a simulation to model surgical robotics is that the model can be used to predict and refine the desired robot parameters before physical implementation. Additionally, experimental outcomes can be reproduced, tested, and optimized for each patient with various trials. In the case where physical testing of the robot on tissue samples or cadavers is unavailable, a simulation of the robot dynamics is also useful. In terms of limitations, biological systems are often nonlinear in nature, and thus difficult to predict solely based on linear models. Another limitation concerns time delays, which are not always ideal in robotic systems. Thus, simulations which make this assumption may be inaccurate. Finally, simulated and physical surgeries utilize different aspects of surgical competency. For instance, communication and fast decision making skills are often vital in physical surgery, but are factors not present within the simulated model.

VI. Conclusion

In this project, the controller-arm dynamics of a simplified model of a surgical robot device and the soft tissue it is meant to operate on were represented as spring-mass-damper systems. To improve the functionality of the device, both a position and force feedback mechanism were implemented into the system. A PID controller was shown to produce the most desired response in terms of accuracy, as the addition of such greatly reduced the steady-state error of the system. Thus, a physical surgical robot may consider the use of a PID controller to specifically aim for an improved accuracy response. A direct future step in regards to the simulation of the model presented in this paper is the addition of a haptic element in order to provide the surgeon with better tactile feedback during operation. The integration of an upgraded impedance control system is also desired to refine the motion control of the surgical robot. While the assumptions and models used in this project reflect a simplified robotic system, the implications of simulating a real surgical robotic system are evident in the ability to predict and control the actual behavior of such systems.

Acknowledgment

We would like to express our gratitude to Professor Cauwenberghs for his passion and dedication in instructing this quarter, especially after a year of online classes. We would also like to thank the TAs, Siwen and Ishan, for consistently providing insight and support during our time in the course.

References

[1] "Robotic surgery: Risks vs. rewards," Patient Safety Network. [Online]. Available: https://psnet.ahrq.gov/web-mm/robotic-surgery-risks-vs-rewards. [Accessed: 09-Dec-2021]

[2] Dong-Won Lim, Eun-Hye Kim, and Yong-Kwun Lee, “Anti-vibration PID control for a robot manipulator experiments,” 2011 8th International Conference on Ubiquitous Robots and Ambient Intelligence (URAI), 2011.
[3] A. M. Okamura, “Haptic feedback in robot-assisted minimally invasive surgery,” Current Opinion in Urology, vol. 19, no. 1, pp. 102–107, 2009.
[4] C. Li, Z. Zhang, G. Xia, X. Xie, and Q. Zhu, “Efficient Force Control Learning System for Industrial Robots Based on Variable Impedance Control,” Sensors, vol. 18, no. 8, p. 2539, Aug. 2018.
[5] P. Moreira, Chao Liu, N. Zemiti, and P. Poignet, “Soft Tissue Force control using active observers and viscoelastic interaction model,” 2012 IEEE International Conference on Robotics and Automation, 2012.
[6] Y. Kobayashi, P. Moreira, C. Liu, P. Poignet, N. Zemiti, and M. G. Fujie, “Haptic feedback control in medical robots through fractional viscoelastic tissue model,” 2011 Annual International Conference of the IEEE Engineering in Medicine and Biology Society, 2011.